Title	Impaired Relaxation in Induced Pluripotent Stem Cell-Derived Cardiomyocytes with Pathogenic TNNI3 Mutation of Pediatric Restrictive Cardiomyopathy
Author(s)	Wang, Renjie; Hasegawa, Moyu; Suginobe, Hidehiro et al.
Citation	Journal of the American Heart Association. 2024, 13(6), p. e032375
Version Type	VoR
URL	https://hdl.handle.net/11094/95638
rights	This article is licensed under a Creative Commons Attribution-NonCommercial 4.0 International License.
Note	

Journal of the American Heart Association

ORIGINAL RESEARCH

Impaired Relaxation in Induced Pluripotent Stem Cell-Derived Cardiomyocytes with Pathogenic *TNNI3* Mutation of Pediatric Restrictive Cardiomyopathy

Renjie Wang ⓘ, MD*; Moyu Hasegawa ⓘ, MD*; Hidehiro Suginobe ⓘ, MD; Chika Yoshihara ⓘ, MD;
Yoichiro Ishii, MD, PhD; Atsuko Ueyama ⓘ, MD; Kazutoshi Ueda, MD; Kazuhisa Hashimoto ⓘ, MD;
Masaki Hirose ⓘ, MD; Ryo Ishii, MD; Jun Narita ⓘ, MD; Takuji Watanabe ⓘ, MD, PhD;
Takuji Kawamura, MD, PhD; Masaki Taira ⓘ, MD; Takayoshi Ueno, MD, PhD; Shigeru Miyagawa ⓘ, MD, PhD;
Hidekazu Ishida ⓘ, MD, PhD

BACKGROUND: Restrictive cardiomyopathy (RCM) is characterized by impaired diastolic function with preserved ventricular contraction. Several pathogenic variants in sarcomere genes, including *TNNI3*, are reported to cause Ca^{2+} hypersensitivity in cardiomyocytes in overexpression models; however, the pathophysiology of induced pluripotent stem cell (iPSC)-derived cardiomyocytes specific to a patient with RCM remains unknown.

METHODS AND RESULTS: We established an iPSC line from a pediatric patient with RCM and a heterozygous *TNNI3* missense variant, c.508C>T (p.Arg170Trp; R170W). We conducted genome editing via CRISPR/Cas9 technology to establish an isogenic correction line harboring wild type *TNNI3* as well as a homozygous *TNNI3*-R170W. iPSCs were then differentiated to cardiomyocytes to compare their cellular physiological, structural, and transcriptomic features. Cardiomyocytes differentiated from heterozygous and homozygous *TNNI3*-R170W iPSC lines demonstrated impaired diastolic function in cell motion analyses as compared with that in cardiomyocytes derived from isogenic-corrected iPSCs and 3 independent healthy iPSC lines. The intracellular Ca^{2+} oscillation and immunocytochemistry of troponin I were not significantly affected in RCM-cardiomyocytes with either heterozygous or homozygous *TNNI3*-R170W. Electron microscopy showed that the myofibril and mitochondrial structures appeared to be unaffected. RNA sequencing revealed that pathways associated with cardiac muscle development and contraction, extracellular matrix-receptor interaction, and transforming growth factor-β were altered in RCM-iPSC-derived cardiomyocytes.

CONCLUSIONS: Patient-specific iPSC-derived cardiomyocytes could effectively represent the diastolic dysfunction of RCM. Myofibril structures including troponin I remained unaffected in the monolayer culture system, although gene expression profiles associated with cardiac muscle functions were altered.

Key Words: cardiomyocytes ■ diastolic dysfunction ■ iPSC ■ isogenic ■ motion analysis ■ restrictive cardiomyopathy

Restrictive cardiomyopathy (RCM) is an extremely rare type of cardiac muscular disease characterized by impaired diastolic function with preserved ventricular contraction. RCM has an annual incidence of approximately 0.04 cases per 10 000 children, accounting for 2% to 5% of pediatric cardiomyopathy.[1]

RESEARCH PERSPECTIVE

What Is New?

- Induced pluripotent stem cell-derived cardiomyocytes from a patient with restrictive cardiomyopathy and a *TNNI3* missense variant R170W present with diastolic dysfunction.
- Genome editing of the *TNNI3* gene completely restored the impaired diastolic function of cardiomyocytes.
- Restrictive cardiomyopathy cardiomyocytes presented with significant alterations in the signaling pathways associated with cardiac muscle contraction, extracellular matrix–focal adhesion interaction, and transforming growth factor-β.

What Question Should Be Addressed Next?

- What specific signaling cascade is responsible for diastolic dysfunction of restrictive cardiomyopathy?
- Could in vivo genome editing be a potential therapeutic strategy for restrictive cardiomyopathy?

Nonstandard Abbreviations and Acronyms

cTnI	cardiac troponin I
HC	healthy control
iPSC	induced pluripotent stem cell
RCM	restrictive cardiomyopathy
TGF	transforming growth factor

The prognosis of pediatric RCM was reported as very poor at >50% postdiagnostic mortality rate within 2 years.[2–5] Evidence is lacking for long-term benefit from drug therapy, and heart transplantation remains the most effective treatment for RCM.[4]

Recent advances in genetics and sequencing technology have enabled the identification of pathogenic and likely-pathogenic variants in approximately 50% of the children with RCM,[6,7] and heterozygous missense variants in sarcomere genes are the most frequently identified of these. The myosin binding protein (*MYBPC3*), β-myosin heavy chain (*MYH7*), myosin light chain (*MYL2*), titin (*TTN*), cardiac troponin I (*TNNI3*), cardiac troponin T (*TNNT2*), and α-cardiac actin (*ACTC*) genes have been associated with pathogenicity of RCM. A recent cohort study indicated that *TNNI3* was the most frequently occurring pathogenic gene in pediatric patients with RCM and that those with pathogenic variants had poorer outcomes than those without any pathogenic variants.[7]

cTnI (cardiac troponin I) encoded by *TNNI3* is an inhibitory subunit of the heterotrimeric troponin complex that plays a key role in inhibiting actin-myosin interaction during diastole. cTnI mutants have been reported to enhance the Ca^{2+} sensitivity of cardiac muscles.[8–10] However, these studies used the recombinant cTnI protein complexed with animal F-actin or transgenic mouse models that did not completely represent the clinical phenotype of RCM. Currently, no published study has focused on the pathophysiology of patient-specific induced pluripotent stem cell (iPSC)-derived cardiomyocytes with *TNNI3* mutations. Therefore, we established an iPSC line from a pediatric patient with RCM and a *TNNI3* heterozygous mutation (c.508C>T; R170W). Additionally, we used clustered regularly interspaced short palindromic repeats (CRISPR)/Cas9 (CRISPR associated protein 9) technology to create isogenic-corrected iPSCs with *TNNI3* (wild type [WT]/WT) and iPSCs with homozygous *TNNI3* (R170W/R170W) mutation to compare the cellular physiology and transcriptomics of differentiated cardiomyocytes.

METHODS

Transparency and Openness Promotion Guidelines Statement

The data that support the findings of this study are available from the corresponding author upon reasonable request.

Institutional Review Board Approval

This study was approved by the Osaka University Clinical Research Review Committee (no. 15211 and no. 442). This investigation conformed to the principles outlined in the Declaration of Helsinki. Written informed consent was obtained from parents of the patients before the harvest of blood mononuclear cells.

Generation of Disease-Specific and Isogenic iPSCs Using CRISPR/Cas9 Genome Editing

Peripheral blood mononuclear cells obtained from a pediatric patient with RCM harboring a heterozygous *TNNI3* mutation (c.508C>T, p.R170W) were provided to establish an iPSC line. Healthy control iPSC lines used in this experiment were generated from 3 independent healthy subjects. Peripheral blood mononuclear cells were separated from peripheral whole blood by using Histopaque (Sigma-Aldrich, St. Louis, MO). Reprogramming was performed by using the CytoTune-iPS 2.1 Sendai Reprogramming Kit (Thermo Fisher Scientific, Waltham, MA). iPSCs were cultured

under feeder-free conditions using StemFit AK02N (AJINOMOTO, Tokyo, Japan) on a laminin-coated plate. Generated iPSCs were confirmed by their pluripotency via immunostaining for OCT3/4, SSEA4, SOX2, and TRA-1-60; the karyotype was also checked. Three germ-layer differentiation was confirmed in vitro by using the Human Pluripotent Stem Cell Functional Identification Kit (R&D Systems, Minneapolis, MN). Goat antihuman Otx2, goat antihuman Brachyury, and goat antihuman SOX17 were used as primary antibodies, with NL557 antigoat IgG as a secondary antibody, to evaluate the ectoderm, mesoderm, and endoderm differentiation, respectively. Nuclei were stained with Hoechst 33342 (1:1000, Dojindo Molecular Technologies, Kumamoto, Japan), and cells were observed using the In Cell Analyzer 6000 (GE Healthcare, Chicago, IL). The missense mutation of c.508C>T in *TNNI3* of established iPSCs was evaluated via Sanger sequencing. We also checked for the presence of residual genes derived from the Sendai virus in the established iPSCs at passage number 9 through quantitative reverse-transcription polymerase chain reaction assay using a commercial primer set (Mr04269880_mr; Thermo Fisher Scientific) and found no Sendai virus incorporation at passage number 9. These iPSCs were applied in further experiments.

Genomic editing was conducted by using CRISPR/Cas9 technology. Briefly, guide RNA was designed with the online tool CRISPRdirect (http://crispr.dbcls.jp) and CRISPOR (http://crispor.tefor.net) to select the CRISPR RNA (homozygous: TAAGGAGTCCCTGGACCTGcGGG/ isogenic-corrected: TAAGGAGTCCCTGGACCTGtGGG). The single-strand oligo donor nucleotide was synthesized (homozygous: 5′-GATCTCTGCAGATGCCATGATGCAGG CGCTGCTGGGGGCCCGGGCTAAGGAGTCCCTGG AtCTGtGGGCCCACCTCAAGCAGGTGAAGAAG GAGGACACCGAGAAGGTGAGTGTGGGCTA AGGCC/isogenic-corrected: 5′-GATCTCTGCAGATGCCA TGATGCAGGCGCTGCTGGGGGCCCGGGCTA AGGAGTCCCTGGAcCTGcGGGCCCA CCTCAAGCAGGTGAAGAAGGAGGACACCGAG AAGGTGAGTGTGGGCTAAGGCC). Cas9 nuclease protein NLS (Nippon gene, Tokyo, Japan) was used as the Cas9 protein. RCM-iPSCs were cultured and fed every 2 days in StemFit medium (Ajinomoto) on iMatrix-511 silk (Matorixome, Suita, Japan)-coated plates at 37 °C and 5% CO_2. Guide RNA and donor DNA were imported to the iPSCs by using the Lonza 4D-Nucleofector System (Lonza, Basel, Switzerland). Genomic-edited iPSCs were seeded into a 6-well plate (Thermo Fisher Scientific), and the quality was checked via polymerase chain reaction-restriction fragment length polymorphism screening. The primer pair (5′-C CTTCGAGGCAAGTTTAAGCGG/5′-CACCCACAGCC CTTCCCCTCAG) and restriction endonuclease BstYI were used for polymerase chain reaction-restriction

fragment length polymorphism screening. Single-cell colony pickup was performed after the quality check. Following repeated sessions of genome editing, iPSC clones were obtained with homozygously repaired alleles or homozygous *TNNI3*-R170W alleles.

Cardiomyocyte Differentiation from iPSCs

All iPSCs were cultured in 6-well plates (Thermo Fisher Scientific) with 1×10^5 cells per well coated with iMatrix-511 silk (Matorixome) for 4 days. StemFit medium (Ajinomoto) with Y-27632 rock inhibitor (S1049, Selleck Chemicals, Houston, TX) was applied for the first 24 hours. Subsequently, CHIR-99021 (13122, Cayman Chemical, Ann Arbor, MI) was applied during the subsequent 48 hours. Then, the culture medium was changed to a chemically defined medium (500 mL of RPMI 1640, 213 μg/mL of L-ascorbic acid, and 500 μg/mL of albumin) with Wnt-C59 (S7037, Selleck Chemicals) applied for next 48 hours. Beating cardiomyocytes were observed around day 8 after initiation of differentiation. Cardiomyocytes were harvested on day 14 and replated into a gelatin-coated 6-well plate at 1×10^6 cells per well and incubated with DMEM (044-29765, FUJIFILM Wako Pure Chemical, Tokyo, Japan) with 10% fetal bovine serum (F7524, Sigma-Aldrich). CHIR (4 μM) and Y-27632 (10 μM) were applied for 24 hours. Media were renewed every 48 hours. All experiments were conducted 28 days after initiating differentiation, and beating cardiomyocytes were observed at least 30 days after initiating differentiation.

Motion Analysis of iPSC-Derived Cardiomyocytes

iPSC-derived cardiomyocytes were replated at day 14 and motion analysis was conducted 28 days after initiating cardiomyocyte differentiation. The SI8000 Cell Motion Imaging System (SONY, Tokyo, Japan) was used to measure the contraction and relaxation of iPSC-derived cardiomyocytes by capturing high-quality videos.[11] Cell movement was converted into a motion vector, and the motion velocity within each region of interest (ROI) was calculated based on the sum of the vector magnitudes. The maximum contraction and relaxation velocity correspond to the contractile and diastolic function of the cardiomyocytes. ROIs were placed to ensure that the beating center of colonies was surrounded and guarantee that each measurement was not affected by more than 1 beating center. Four-hundred ROIs were analyzed in each line of iPSC-derived cardiomyocytes. Video imaging of beating iPSC-cardiomyocytes was recorded for 15 seconds at 150 frames per second, a resolution of 1024×1024 pixels, and a depth of 8 bits using a ×4 objective lens. Motion vectors were analyzed with SI8000 Analyze software.

Ca²⁺ Oscillation

On day 28 after differentiation, the medium was changed to the recording medium, containing Calcium Kit Fluo-4 (Dojindo) dissolved in dimethyl sulfoxide with 1.25 mmol/L probenecid and 0.04% Pluronic F-127, according to the manufacturer's instructions. All cardiomyocyte lines were cultured for 1 hour in the recording media, and then the media were changed to recording media with 1.25 mmol/L probenecid. Ca²⁺ oscillation indicated by Fluo-4 fluorescence was observed using a FV3000 microscope (Olympus, Tokyo, Japan) with a ×20 objective lens. Time-lapse video imaging was recorded for 5 seconds at a resolution of 128×128 pixels. Nine isolated iPS-cardiomyocytes were analyzed in each iPSC-derived cardiomyocyte line.

Immunocytochemistry

On day 28 after differentiation, all cardiomyocyte lines were seeded on gelatin-coated glass coverslips cultured with DMEM/10% fetal bovine serum with Y-27632 for 24 hours. Immunostaining was performed using goat anti-cTnI (Abcam, ab56357; 1:300) and rabbit anti-cTnT (cardiac troponin T; Abcam, ab209813; 1:300) as primary antibodies and Alexa Fluor 488 donkey antigoat IgG (Thermo Fisher Scientific, A11055; 1:500) and Alexa Fluor 647 donkey antirabbit IgG (Thermo Fisher Scientific, A31573; 1:500) as secondary antibodies. Cells were washed with PBS, fixed with 4% paraformaldehyde for 15 minutes, and permeabilized with PBS containing 0.5% Triton-X-100 (Sigma-Aldrich) for 15 minutes. Cells were then blocked with 5% fetal bovine serum in PBS for 30 minutes and were subsequently incubated overnight at 4 °C with primary antibodies. The following day, secondary antibodies and Hoechst 33342 (1:1000, Dojindo) were used to visualize the primary antibodies and nuclei, respectively. After immunostaining was completed, glass coverslips were stuck to slide glasses with ProLong Gold antifade reagent (P10144, Thermo Fisher Scientific). Cells were observed using a FV3000 microscope (Olympus) with a ×100 objective lens.

Flow Cytometry

Flow cytometry was conducted on day 14 of cardiomyocyte differentiation to determine cardiomyocyte purity and on day 28 to determine the cardiomyocyte subtype. Briefly, the cells were dissociated using TrypLE Select Enzyme (12563011, Thermo Fisher Scientific) and collected in DMEM with 10% fetal bovine serum. The cell suspension was aliquoted into round-bottomed polystyrene test tubes (352235, Corning, Glendale, CA), with 5×10⁵ cells per tube. The BD Cytofix/Cytoperm Fixation/Permeabilization Kit (554714, BD Biosciences, Franklin Lakes, NJ) was used to fix the cells in accordance with the manufacturer's instructions. Permeabilization was conducted by using 0.1% Triton-X for MLC2v (myosin light chain 2v) and 0.5% Triton-X for cTnT, MLC2a, and HCN4. Immunostaining was performed with rabbit anti-cTnT (Abcam, ab209813; 1:300), rabbit anti-MLC2v (Proteintech, 10906-1-AP; 1:300), mouse anti-MLC2a (Synaptic Systems, 311011; 1:300), and mouse anti-HCM4 (Abcam, ab302675; 1:300) as the primary antibodies. Alexa Fluor 647 donkey antirabbit and antimouse IgG antibodies (Thermo Fisher Scientific, A31573 and A31571; 1:500) were used as the secondary antibodies. Cells were incubated overnight with primary antibodies at 4 °C. The secondary antibodies were applied for 30 minutes at 4 °C. Flow cytometry was performed using BD FACSCanto II System (BD Biosciences) and the results were analyzed using FlowJo software (BD Biosciences).

Electron Microscope Observation

All iPSC-derived cardiomyocyte lines were observed using a transmission electron microscope (HT7800; Hitachi, Tokyo, Japan). On day 28 after differentiation, cells were fixed with 2.5% glutaraldehyde in 0.1 M sodium phosphate buffer in double-distilled water. Cells were dehydrated through graded concentrations of ethanol and propylene oxide and subsequently embedded in Quetol-812 (Nisshin-EM, Tokyo, Japan). Ultrathin sections were cut from blocks and mounted on copper grids.

RNA Sequencing

Total RNA was extracted from all cardiomyocytes lines with a Nucleospin RNA column kit (TakaraBio). Library preparation was performed as previously described.[11] Sequencing was performed on an Illumina HiSeq 2500 platform in 75-base single-end mode; Illumina CASAVA 1.8.2 software was used for base calling. Sequenced reads were mapped to the human reference genome sequence (hg 19) using TopHat ver. 2.0.13 in combination with Bowtie2 ver. 2.2.3 and SAMtools ver. 0.1.19. Fragments per kilobase of exon per million mapped fragments were calculated using Cuffnorm ver. 2.2.1. Ingenuity pathway analysis was used to identify canonical pathways from differentially expressed genes. Data from this study can be accessed under Gene Expression Omnibus experiment accession number (GSE240775). Transcriptomes were analyzed using the integrated differential expression and pathway platform analysis (http://bioinformatics.sdstate.edu/idep96/) and Subio (Subio Inc, Japan) platforms. A list of the enriched Kyoto Encyclopedia of Genes and Genomes pathways were obtained using the DAVID functional annotation web tool (https://david-d.ncifcrf.gov).

Statistical Analysis

All statistical analyses were performed using JMPpro17 (SAS Institute, Cary, NC). First, the Shapiro–Wilk test was conducted to evaluate normal distributions. Equality of variance was evaluated using the Bartlett or Levene test. Statistical comparisons among multiple groups were performed using a one-way analysis of variance when the normality and homogeneity of variance were confirmed. Otherwise, the Kruskal–Wallis test was performed. Thereafter, the Tukey–Kramer or Steel–Dwass test was conducted to compare the groups. A P value of <0.01 was considered to be statistically significant.

RESULTS

Clinical Characterization

A male patient was diagnosed with idiopathic RCM at 2 years old due to congestive heart failure symptoms. The patient received a ventricular assist device at 3 years old and heart transplantation at 4 years old. The patient had no history of ventricular arrhythmia and no family history. Whole exome sequencing revealed a heterozygous missense variant of c.508C>T (p.Arg170Trp; R170W) in *TNNI3*, which was previously reported as a causative variant for pediatric RCM.[9] Blood mononuclear cells for the establishment of an iPSC line were obtained when the patient was 4 years old. The echocardiography at diagnosis and histological findings of the left ventricle are presented at Figure S1.

Establishment of iPSC Lines and Cardiomyocyte Differentiation

Using CytoTune-iPS 2.0 Sendai Reprogramming Kit, we generated iPSC lines from the patient harboring the heterozygous missense variant (c.508C>T) of *TNNI3* (Hetero-iPSC). We validated the quality of the iPSCs by checking the pluripotent markers, karyotype, and three germ-layer differentiation and by direct Sanger sequencing of *TNNI3* (Figure S2). Three lines of healthy control iPSCs (HC1-, HC2-, and HC3-iPSCs) were also used. To exclude the possibility of interindividual variability, we conducted genomic editing for *TNNI3* by using CRISPR/Cas9 technology to correct the RCM-iPSC line to the WT *TNNI3* (isogenic-corrected WT control: WT-iPSC). Moreover, to evaluate the severity of the phenotype in cardiomyocytes with homozygous *TNNI3* mutation, we used CRISPR/Cas9 to generate an isogenic homogyzous *TNNI3*-R170W line (Homo-iPSC).

Then, all iPSC lines were differentiated to cardiomyocytes by using the defined monolayer method. Purities of cardiomyocytes were determined by using flow cytometry for cTnT, and were confirmed to be >90% for all iPSC lines (Figure S3A and S3B). Among these, approximately 60% to 80% of the differentiated cardiomyocytes were identified as MLC2v-positive ventricular cardiomyocytes. The remaining 20% to 40% of the cells were MLC2a positive atrial or immature ventricular cardiomyocytes. Only 5% to 10% of the cells were HCN4-positive conduction system cardiomyocytes. Notably, there were no significant differences in the MLC2v-, MLC2a-, and HCN4-positive ratios among the lines of iPSC-derived cardiomyocytes (Figure S3C and S3D). All differentiated cardiomyocytes showed spontaneous beating until differentiation day 14.

Motion Analysis

To investigate the contractile and relaxation function of iPSC-derived cardiomyocytes, we used a Sony SI8000 motion analyzer to evaluate the motion vectors of the beating cardiomyocytes as this can quantitatively represent the electrophysiological and functional characteristics of cardiomyocytes.[12] We analyzed both the contraction and relaxation velocities and their durations in 400 ROIs set around the beating colonies of cardiomyocytes. Before analyses, we replated the beating cardiomyocytes at day 14 from the initiation of differentiation and settled the cells for more than 14 days to standardize the size of the cardiomyocyte beating clusters in each line (Video S1). However, there were still large variations in the velocities and durations of each ROI (Figure S4). Therefore, we calculated the relaxation velocity/contraction velocity ratio and the relaxation duration/contraction duration ratio to compensate for the variation of beating in cardiomyocytes (Figure 1A). The relaxation velocity/contraction velocity in Hetero-cardiomyocytes and Homo-cardiomyocytes were significantly impaired compared with that in HC-cardiomyocytes (Figure 1B and 1C). The isogenic genomic correction line of WT-cardiomyocytes harboring WT-*TNNI3* showed similar relaxation velocity/contraction velocity and relaxation duration/contraction duration ratios seen in HC-cardiomyocytes, suggesting that *TNNI3* editing could completely restore the diastolic dysfunction of RCM. Moreover, Homo-cardiomyocytes had a significantly lower relaxation velocity/contraction velocity ratio and a higher relaxation duration/contraction duration ratio than those of Hetero-cardiomyocytes, indicating that Homo-cardiomyocytes exhibited a severer phenotype compared with that in the heterozygous R170W mutant cardiomyocytes.

Ca²⁺ Oscillation

To evaluate the intracellular Ca^{2+} kinetics in RCM-cardiomyocytes, we used Fluo 4-AM to visualize Ca^{2+} oscillation. The optical densities of the cells were recorded and analyzed, as presented in Figure 2A. The
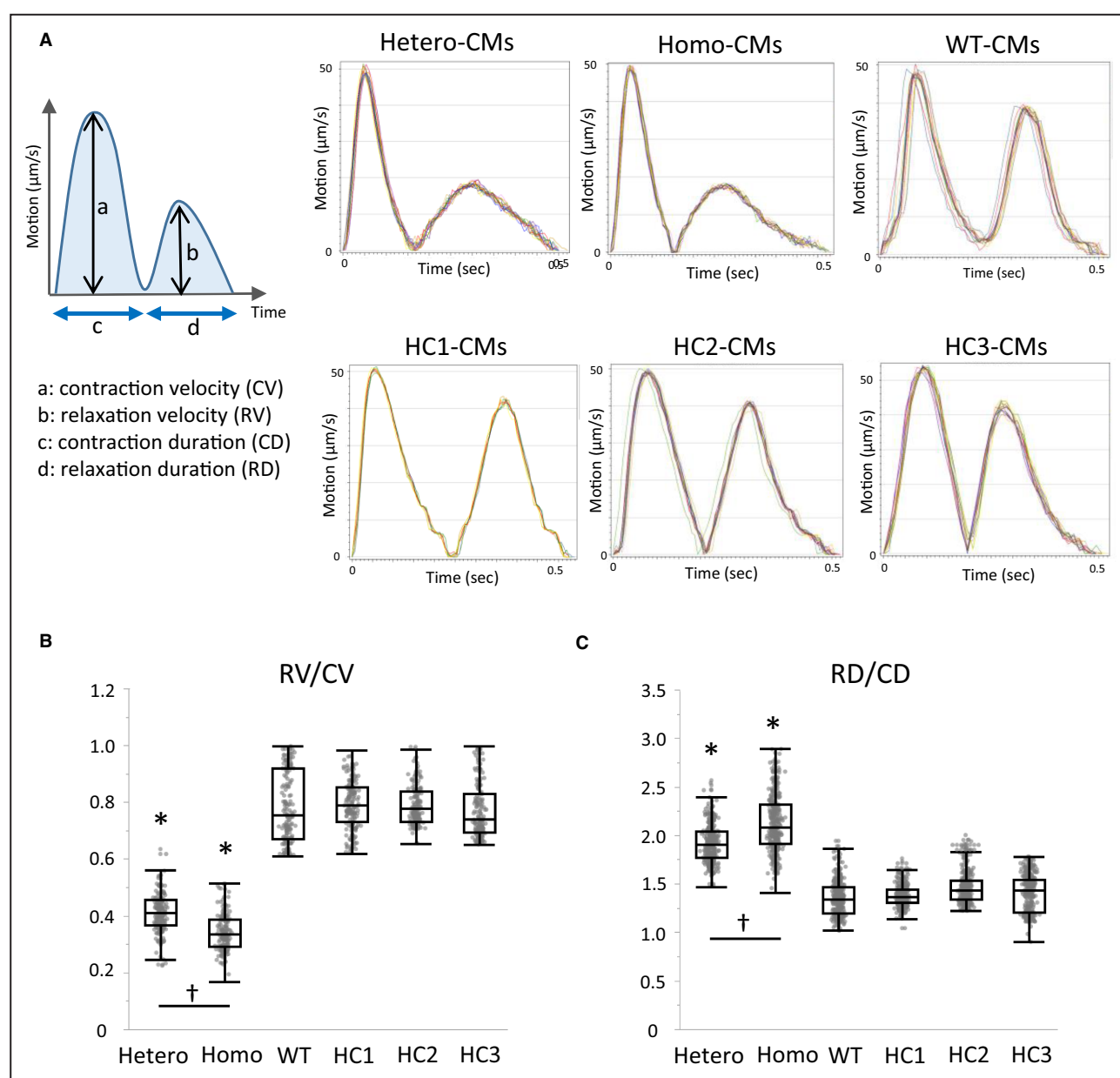
Figure 1.   Motion vector analysis for induced pluripotent stem cell-derived cardiomyocytes.
A, Representative images of motion waveform representing cardiomyocyte contraction and relaxation. **B**, Quantitative analysis for the ratio of relaxation peak velocity (RV) and contraction peak velocity (CV). **C**, Quantitative analysis for the ratio of relaxation duration (RD) and contraction duration (CD). N=400 in each analysis. Tukey–Kramer multiple comparison test was conducted. *$P<0.001$ versus WT, HC1, HC2, and HC3. †$P<0.01$ between Hetero-CMs and Homo-CMs. CM indicates cardiomyocyte; HC, healthy control; Hetero, heterozygous; Homo, homozygous; and WT, wild type.

beating rates of each cardiomyocyte group did not significantly differ. No significant differences were found in the amplitude of oscillation, Ca^{2+} recovery velocity, and Ca^{2+} uptake velocity among Hetero-cardiomyocytes, Homo-cardiomyocytes, WT-cardiomyocytes, or HC-cardiomyocytes (Figure 2B–D), suggesting that intracellular Ca^{2+} kinetics, which is mainly controlled by L-type Ca^{2+} channels and the sarcoplasmic reticulum, was unaffected in RCM-iPSC-derived cardiomyocytes with the *TNNI3* variant.

Immunocytochemistry of Troponin Complex

To visualize the intracellular localization and structures of cTnI-R170W in cardiomyocytes, we analyzed the immunocytochemistry of cTnI and cTnT in iPSC-derived cardiomyocytes. cTnI-R170W colocalized with cTnT even in Hetero-cardiomyocytes and Homo-cardiomyocytes, which was similar to that observed with HC-cardiomyocytes and WT-cardiomyocytes
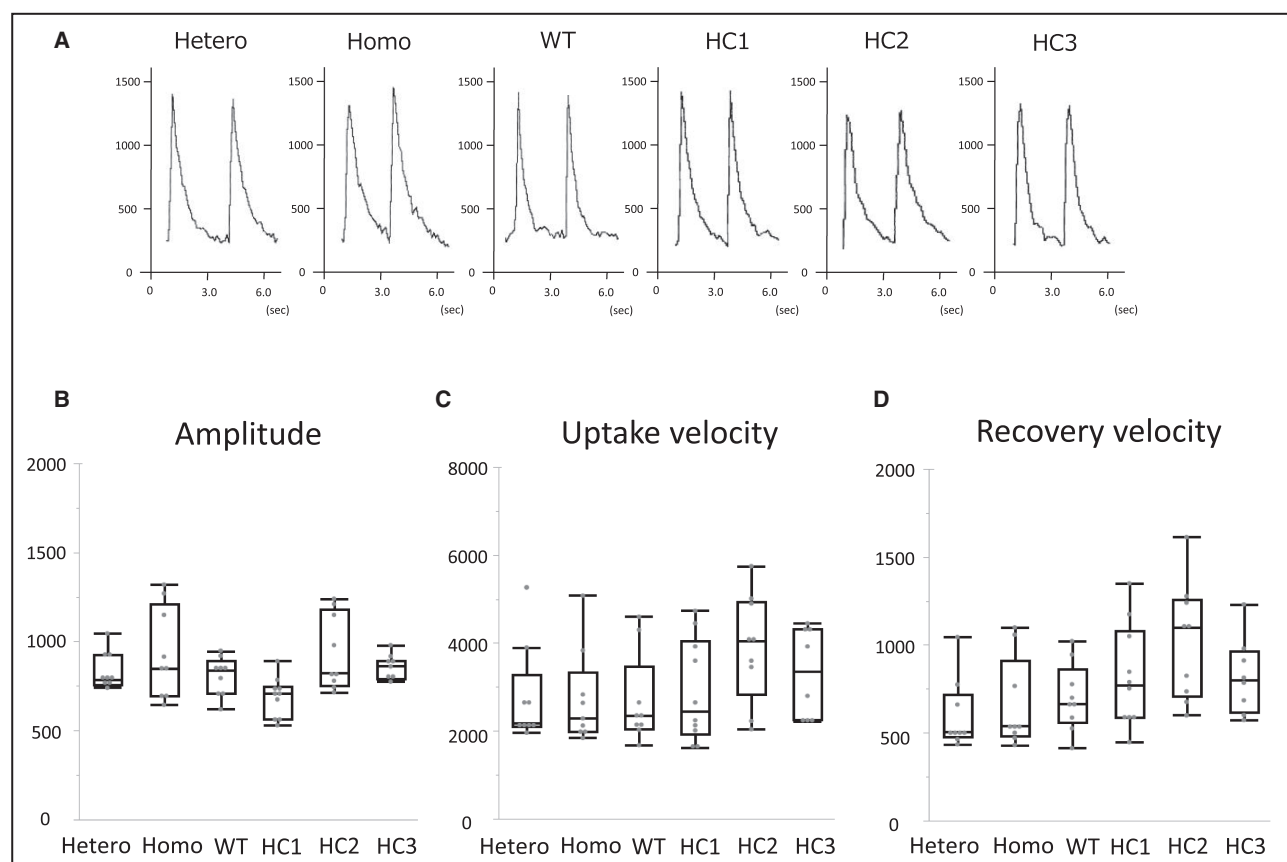
Figure 2.   Ca²⁺ oscillation analysis in iPSC-derived cardiomyocytes assessed via Fluo-4 imaging.
A, Representative images of Ca²⁺ oscillation. **B**, Amplitude of iPSC-derived CMs. **C**, Ca²⁺ uptake velocity of iPSC-derived CMs. **D**, Ca²⁺ recovery velocity of iPSC-derived CMs. No significant differences were observed among each cardiomyocyte type using Steel–Dwass multiple comparison tests. CM indicates cardiomyocyte; HC, healthy control; Hetero, heterozygous; Homo, homozygous; iPSC, induced pluripotent stem cell; and WT, wild type.

(Figure 3). Moreover, the typical striated structures of cardiomyocytes did not significantly differ among Hetero-cardiomyocytes, Homo-cardiomyocytes, WT-cardiomyocytes, or HC-cardiomyocytes. We could not find any misalignment of cTnI in either Hetero-cardiomyocytes or Homo-cardiomyocytes. This result suggests that mutant cTnI successfully formed a troponin complex with cTnT.

Electron Microscope Observation

Because the formation of the troponin complex was unaffected in both Hetero-cardiomyocytes and Homo-cardiomyocytes, we used electron microscopy to observe the myofibril structures and mitochondrial morphologies. We first evaluated the left ventricle free wall in the harvested heart of the patient with RCM and could not find any disarrayed myofibrils or z-disks (Figure 4A). We then analyzed the iPSC-derived cardiomyocytes. Myofibrils did not exhibit any apparent disarray in Hetero-cardiomyocytes or in Homo-cardiomyocytes compared with that in WT-cardiomyocytes and HC-cardiomyocytes (Figure 4B),

although the density of myofibril structures in iPSC-derived cardiomyocytes was sparser than that in tissue samples from the patient's heart. Mitochondrial structures did not significantly differ among the iPSC-derived cardiomyocyte lines and were similar to that in the tissue sample the patient's left ventricular.

RNA Sequencing

Finally, we used RNA sequencing of differentiated cardiomyocytes to investigate the specific signaling pathway in RCM-cardiomyocytes. A heat map analysis of the top 3000 genes revealed distinct expression patterns in Hetero-cardiomyocytes and Homo-cardiomyocytes compared with those in WT-cardiomyocytes and HC-cardiomyocytes (Figure 5A). K-means clustering divided the top 2000 genes into 4 groups that exhibited similar distinctive expression patterns (Figure 5B). T-distributed stochastic neighbor embedding analysis indicated distinct grouping of Hetero- and Homo-cardiomyocytes and of WT- and HC-cardiomyocytes (Figure 5C). A gene ontology analysis revealed that the pathways associated were muscular system development,
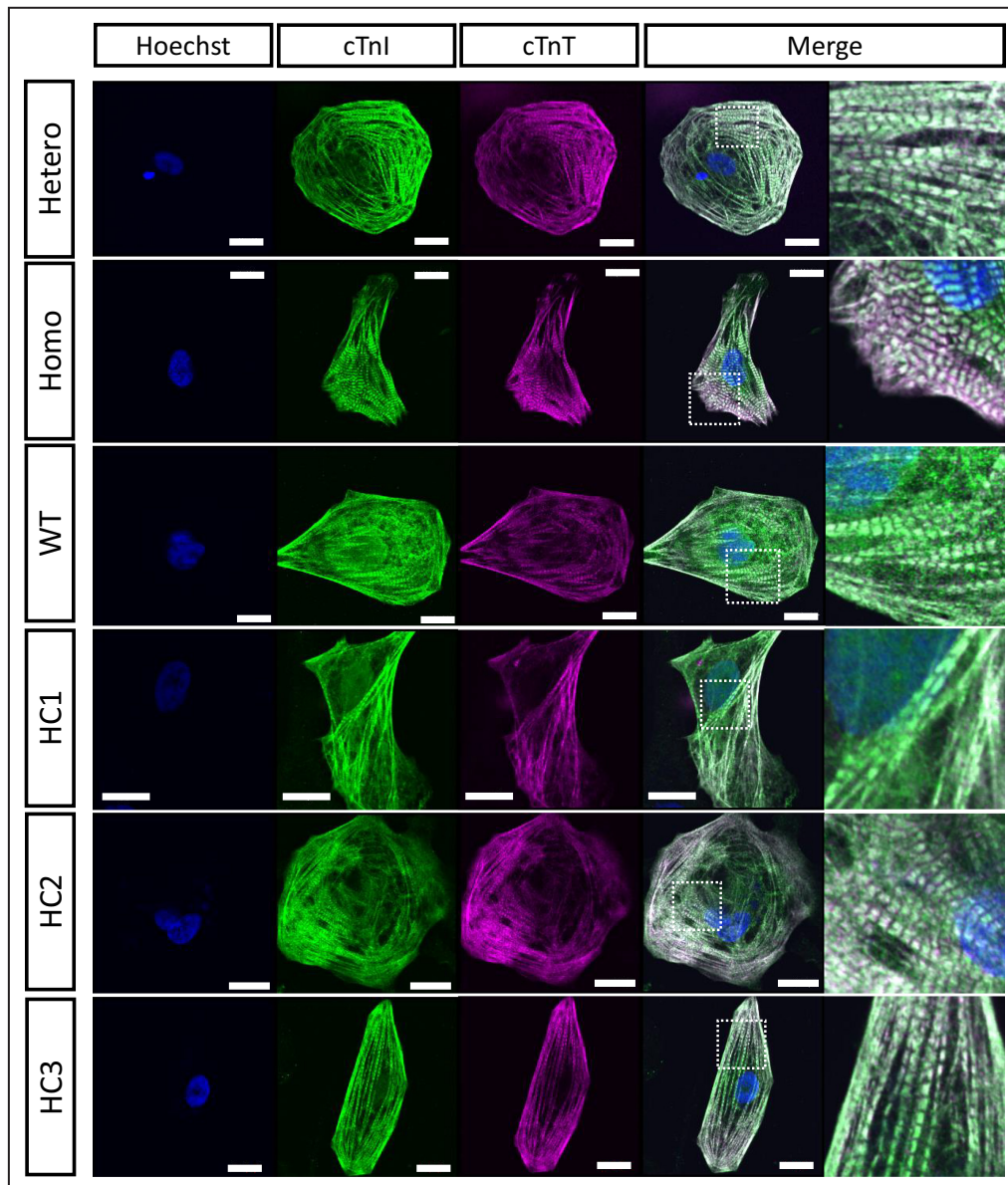
**Figure 3. Immunocytochemistry for cardiac troponin I and cardiac troponin T.**
Nuclei were counterstained with Hoechst 33342. All iPSC-derived CMs were stained with a typical striated pattern for cTnI and cTnT. Scale bar: 20 μm. cTnI indicates cardiac troponin I; cTnT, cardiac troponin T; HC, healthy control; Hetero, heterozygous; Homo, homozygous; and WT, wild type.

vasculature development, response to cytokines, and extracellular structure organization were enriched in each cluster (Figure S5). Finally, we performed pathway analyses to determine which particular signaling pathways influenced the diastolic dysfunction of RCM-cardiomyocytes. Extracellular matrix (ECM)–receptor interactions ($P=0.00016$) and cardiac muscle contraction ($P<0.0001$) were found to be considerably active in Hetero- and Homo-cardiomyocytes. Furthermore, the TGF-β (transforming growth factor-β) pathway ($P=0.00082$) was substantially altered (Figure S6). The specific gene expression panel revealed alterations in the expression of multiple genes associated with the identified pathways (Figure S7).

DISCUSSION

Pediatric RCM is a rare disease with an extremely poor prognosis. Because no effective medications are available for RCM, analysis of the molecular pathogenesis is urgently required. Genetic studies revealed that the cardiomyocytes of approximately 50% of pediatric patients with RCM carry gene mutations in *TNNI3*, *TNNT2*, *MYL2*, *MYH7*, *MYBPC3*, and *ACTC1*.[6,7] Herein,
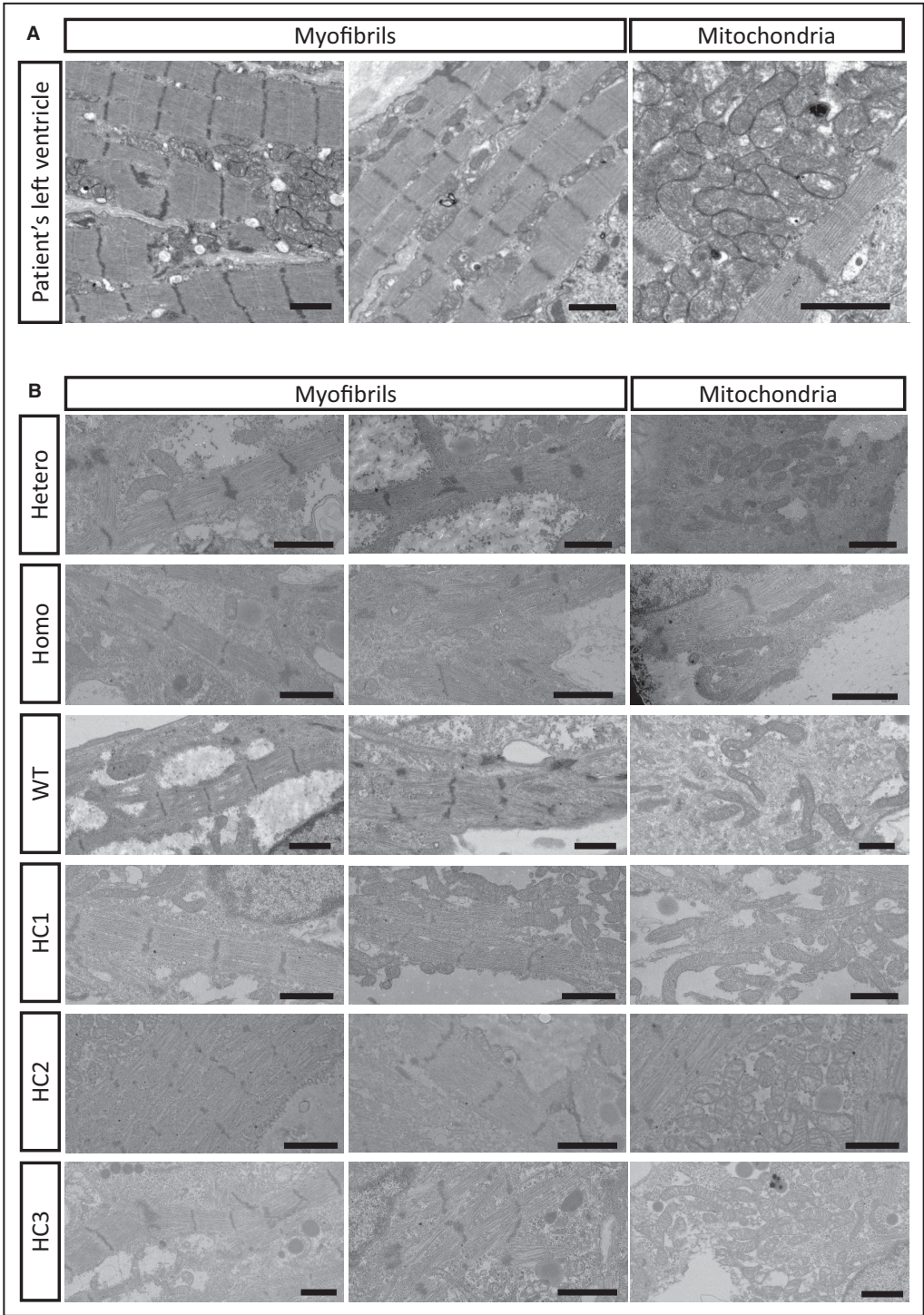
Figure 4. Electron microscopy imaging of patient tissue sample and iPSC-derived cardiomyocytes.
A, Electron microscopy imaging of the left ventricle tissue harvested at heart transplantation from the patient with restrictive cardiomyopathy. **B**, Electron microscopy imaging of iPSC-derived CMs. Scale bar: 1 μm. CM indicates cardiomyocyte; HC, healthy control; Hetero, heterozygous; Homo, homozygous; iPSC, induced pluripotent stem cell; and WT, wild type.

we showed diastolic dysfunction of cardiomyocytes derived from iPSC of patients with RCM with heterozygous cTnI-R170W and genomic-edited cardiomyocytes with homozygous cTnI-R170W. We clearly demonstrated that the genomic correction of cTnI-R170W to WT cTnI completely restored the diastolic dysfunction.
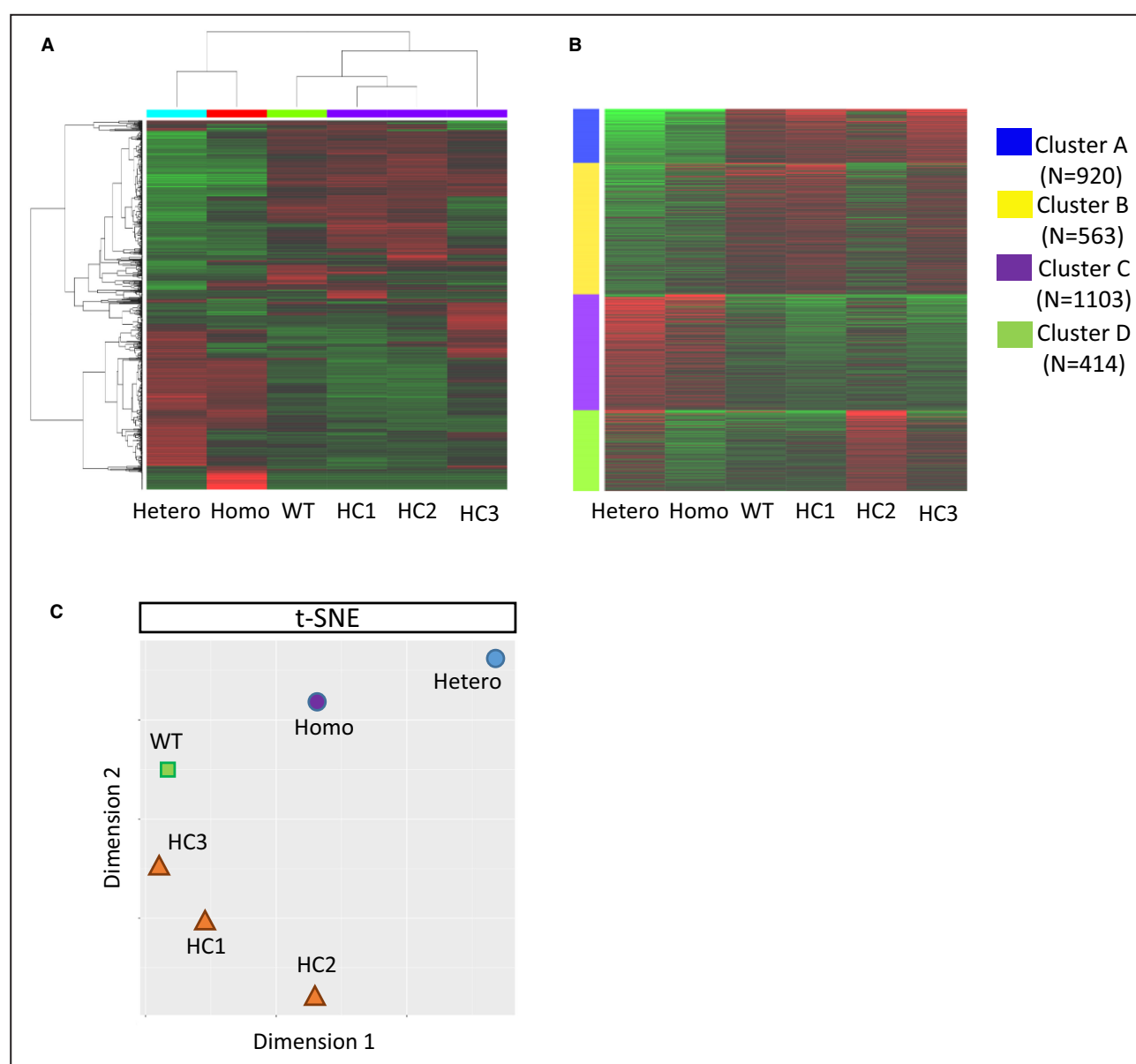
Figure 5.   RNA-sequencing analyses of iPSC-derived cardiomyocytes.
A, Hierarchical clustering of RNA sequencing in each iPSC-derived cardiomyocyte group. **B**, K-means clustering analysis of the top 2000 differentially expressed genes. **C**, T-distributed stochastic neighbor embedding (t-SNE) analysis of RNA sequencing. HC indicates healthy control; Hetero, heterozygous; Homo, homozygous; iPSC, induced pluripotent stem cell; and WT, wild type.

Moreover, the homozygous cTnI-R170W cardiomyocytes exhibited a significantly more severe phenotype than that of heterozygous cTnI-R170W. These results can reduce the possibility of interindividual errors of phenotype of iPSC-derived cardiomyocytes.

One of the most important limitations using iPSC-derived cardiomyocytes for pathogenic analysis for cardiomyopathy is their maturation. iPSC-derived cardiomyocytes exhibit immature features similar to fetal or infantile cardiomyocytes in human hearts.[13] The myofibril alignment, electrophysiology, Ca^{2+} handling, cell cycle, and metabolism significantly differ between immature and mature cardiomyocytes. To facilitate iPSC-derived cardiomyocyte maturation, we cultured them for 28 days after cardiomyocyte differentiation was initiated. We consider that the adult phenotype of cardiomyocytes cannot be reached in such a culture duration. However, the patient of R170W did exhibit heart failure as an infant; therefore, we could demonstrate the phenotypes of iPSC-derived cardiomyocytes in this study.

The mutants of cTnT and cTnI associated with RCM have been reported to show hypersensitivity to Ca^{2+} by overexpressing recombinant proteins in skinned fibers

or myofibers derived from the transgenic mice.[8,10,14–16] More recently, Cimiotti et al reported that the cTnI-R170W mutation demonstrated Ca^{2+} hypersensitivity and disintegration of thin filaments by using a recombinant mutant protein of cTnI and other troponin complex proteins.[9] By contrast, Ca^{2+} concentration in cardiomyocytes is regulated by the Ca^{2+} channels in plasma membrane and by RYR2 and SERCA2 in the sarcoplasmic reticulum.[17] As we expected, the amplitude, uptake velocity, and recovery velocity of Ca^{2+} oscillation did not significantly vary among Hetero-cardiomyocytes, Homo-cardiomyocytes, WT-cardiomyocytes, or HC-cardiomyocytes. Therefore, we speculate that Ca^{2+} kinetics is not associated with the pathogenesis of RCM. However, the recent study for of iPSC-derived cardiomyocytes with an in-frame deletion of *FLNC* showed impaired relaxation and reduced Ca^{2+} kinetics.[18] We could not determine why this discrepancy occurs, although we speculate that differences between pathogenic genes (*TNNI3* versus *FLNC*) may affect the results.

We used immunocytochemistry and electron microscopy to analyze the structural changes of myofibrils in RCM-cardiomyocytes. The immunocytochemistry of cTnI and cTnT suggests that the troponin complex is normally formed in the sarcomere and that degradation and misalignment of cTnI is not the cause of RCM. Moreover, we could not find any apparent disarray of myofibrils either in Hetero-cardiomyocytes or Homo-cardiomyocytes as compared with myofibrils in WT-cardiomyocytes and HC-cardiomyocytes. A study using the recombinant protein of cTnI-R170W showed that the thin filament formation was slightly disturbed.[9] We could not clearly uncover how this discrepancy occurred, although overexpression of the recombinant protein by *Escherichia coli* and subsequent purification procedures may affect the results. We also demonstrated that the electron microscope assessment of the patient's heart tissues were similar to those of our iPSC-derived cardiomyocytes.

Finally, we revealed that the comprehensive expression profiles of Hetero-cardiomyocytes and Homo-cardiomyocytes were clearly distinct from those of isogenic WT-cardiomyocytes and HC-cardiomyocytes. Gene ontology analysis revealed that the heterozygous and homozygous mutations of cTnI-R170W influence the molecular signaling pathways associated with muscle development and contraction, vasculature development, cytokine responses, and ECMs. Moreover, further pathway analyses demonstrated that not only cardiac muscle-related genes but also ECM–receptor and focal adhesion interactions and TGF-β signaling pathway were significantly affected in RCM-cardiomyocytes. Increased focal adhesion and ECM proteins may alter cell–cell interactions and affect the diastolic behaviors of cardiomyocytes.[19] TGF-β signaling is reported to be activated in experimental models of myocardial infarction, cardiac hypertrophy, and in human patients with cardiomyopathy.[20,21] TGF-β signaling is also involved in cardiac fibrosis and fibroblast activation.[22] We cannot reveal the precise mechanism by which sarcomere genes, including cardiac actin, myosin heavy and light chains, and troponins T and C, are upregulated in RCM-cardiomyocytes. However, sarcomere gene expression has been demonstrated to be elevated in failing hearts with cardiomyopathy.[23] The increased cardiomyocyte stress might lead to the expression of various cardiac muscle-related genes to compensate for the dysfunction.

Although we could not determine which specific signaling pathway was the most important for RCM pathogenesis, these alterations in gene expression profiles in cytokine responses and ECMs indicate that cell–cell communication among RCM-cardiomyocytes could be a possible pathogenic mechanism of RCM. Further studies are warranted to identify which specific signaling molecules are responsible for RCM pathogenesis and represent potential therapeutic targets.

CONCLUSIONS

RCM patient-specific iPSC-derived cardiomyocytes were shown to demonstrate the diastolic dysfunction of RCM. Although myofibril structures and Ca^{2+} kinetics were not significantly affected in RCM-cardiomyocytes, gene expression profiles were shown to be clearly distinct compared with those of control cardiomyocytes. The genomic editing of the *TNNI3* mutation completely restored the diastolic function and gene expression patterns of RCM-cardiomyocytes.

Affiliations

Department of Pediatrics (R.W., H.S., C.Y., A.U., K.U., K.H., M. Hirose, R.I., J.N., H.I.) and Department of Cardiovascular Surgery (M. Hasegawa, T.W., T.K., M.T., T.U., S.M.), Osaka University Graduate School of Medicine, Osaka, Japan; and Department of Pediatric Cardiology, Osaka Children's and Women's Hospital, Osaka, Japan (Y.I.).

Supplemental Material

Figures S1–S7
Video S1

REFERENCES

1. Lee TM, Hsu DT, Kantor P, Towbin JA, Ware SM, Colan SD, Chung WK, Jefferies JL, Rossano JW, Castleberry CD, et al. Pediatric

cardiomyopathies. *Circ Res*. 2017;121:855–873. doi: 10.1161/CIRCRESAHA.116.309386

2. Webber SA, Lipshultz SE, Sleeper LA, Lu M, Wilkinson JD, Addonizio LJ, Canter CE, Colan SD, Everitt MD, Jefferies JL, et al. Outcomes of restrictive cardiomyopathy in childhood and the influence of phenotype: a report from the pediatric cardiomyopathy registry. *Circulation*. 2012;126:1237–1244. doi: 10.1161/CIRCULATIONAHA.112.104638

3. Anderson HN, Cetta F, Driscoll DJ, Olson TM, Ackerman MJ, Johnson JN. Idiopathic restrictive cardiomyopathy in children and young adults. *Am J Cardiol*. 2018;121:1266–1270. doi: 10.1016/j.amjcard.2018.01.045

4. Wittekind SG, Ryan TD, Gao Z, Zafar F, Czosek RJ, Chin CW, Jefferies JL. Contemporary outcomes of pediatric restrictive cardiomyopathy: a single-center experience. *Pediatr Cardiol*. 2019;40:694–704. doi: 10.1007/s00246-018-2043-0

5. Mori H, Kogaki S, Ishida H, Yoshikawa T, Shindo T, Inuzuka R, Furutani Y, Ishido M, Nakanishi T. Outcomes of restrictive cardiomyopathy in Japanese children- a retrospective cohort study. *Circ J*. 2022;86:1943–1949. doi: 10.1253/circj.CJ-21-0706

6. Kostareva A, Kiselev A, Gudkova A, Frishman G, Ruepp A, Frishman D, Smolina N, Tarnovskaya S, Nilsson D, Zlotina A, et al. Genetic spectrum of idiopathic restrictive cardiomyopathy uncovered by next-generation sequencing. *PLoS One*. 2016;11:e0163362. doi: 10.1371/journal.pone.0163362

7. Ishida H, Narita J, Ishii R, Suginobe H, Tsuru H, Wang R, Yoshihara C, Ueyama A, Ueda K, Hirose M, et al. Clinical outcomes and genetic analyses of restrictive cardiomyopathy in children. *Circ Genom Precis Med*. 2023;16:382–389. doi: 10.1161/CIRCGEN.122.004054

8. Wen Y, Xu Y, Wang Y, Pinto JR, Potter JD, Kerrick WG. Functional effects of a restrictive-cardiomyopathy-linked cardiac troponin I mutation (R145W) in transgenic mice. *J Mol Biol*. 2009;392:1158–1167. doi: 10.1016/j.jmb.2009.07.080

9. Cimiotti D, Fujita Becker S, Möhner D, Smolina N, Budde H, Wies A, Morgenstern L, Gudkova A, Sejersen T, Sjöberg G, et al. Infantile restrictive cardiomyopathy: cTnI-R170G/W impair the interplay of sarcomeric proteins and the integrity of thin filaments. *PLoS One*. 2020;15:e0229227. doi: 10.1371/journal.pone.0229227

10. Pinto JR, Parvatiyar MS, Jones MA, Liang J, Potter JD. A troponin T mutation that causes infantile restrictive cardiomyopathy increases Ca2+ sensitivity of force development and impairs the inhibitory properties of troponin. *J Biol Chem*. 2008;283:2156–2166. doi: 10.1074/jbc.M707066200

11. Tsuru H, Ishida H, Narita J, Ishii R, Suginobe H, Ishii Y, Wang R, Kogaki S, Taira M, Ueno T, et al. Cardiac fibroblasts play pathogenic roles in idiopathic restrictive cardiomyopathy. *Circ J*. 2021;85:677–686. doi: 10.1253/circj.CJ-20-1008

12. Hayakawa T, Kunihiro T, Ando T, Kobayashi S, Matsui E, Yada H, Kanda Y, Kurokawa J, Furukawa T. Image-based evaluation of contraction-relaxation kinetics of human-induced pluripotent stem cell-derived cardiomyocytes: correlation and complementarity with extracellular electrophysiology. *J Mol Cell Cardiol*. 2014;77:178–191. doi: 10.1016/j.yjmcc.2014.09.010

13. Karbassi E, Fenix A, Marchiano S, Muraoka N, Nakamura K, Yang X, Murry CE. Cardiomyocyte maturation: advances in knowledge and implications for regenerative medicine. *Nat Rev Cardiol*. 2020;17:341–359. doi: 10.1038/s41569-019-0331-x

14. Yumoto F, Lu QW, Morimoto S, Tanaka H, Kono N, Nagata K, Ojima T, Takahashi Yanaga F, Miwa Y, Sasaguri T, et al. Drastic Ca2+ sensitization of myofilament associated with a small structural change in troponin I in inherited restrictive cardiomyopathy. *Biochem Biophys Res Commun*. 2005;338:1519–1526. doi: 10.1016/j.bbrc.2005.10.116

15. Gomes AV, Liang J, Potter JD. Mutations in human cardiac troponin I that are associated with restrictive cardiomyopathy affect basal ATPase activity and the calcium sensitivity of force development. *J Biol Chem*. 2005;280:30909–30915. doi: 10.1074/jbc.M500287200

16. Davis J, Wen H, Edwards T, Metzger JM. Allele and species dependent contractile defects by restrictive and hypertrophic cardiomyopathy-linked troponin I mutants. *J Mol Cell Cardiol*. 2008;44:891–904. doi: 10.1016/j.yjmcc.2008.02.274

17. Federico M, Valverde CA, Mattiazzi A, Palomeque J. Unbalance between sarcoplasmic reticulum Ca2+ uptake and release: a first step toward Ca2+ triggered arrhythmias and cardiac damage. *Front Physiol*. 2019;10:1630. doi: 10.3389/fphys.2019.01630

18. Wang BZ, Nash TR, Zhang X, Rao J, Abriola L, Kim Y, Zakharov S, Kim M, Luo LJ, Morsink M, et al. Engineered cardiac tissue model of restrictive cardiomyopathy for drug discovery. *Cell Rep Med*. 2023;4:100976. doi: 10.1016/j.xcrm.2023.100976

19. Talior-Volodarsky I, Connelly KA, Arora PD, Gullberg D, McCulloch CA. Alpha11 integrin stimulates myofibroblast differentiation in diabetic cardiomyopathy. *Cardiovasc Res*. 2012;96:265–275. doi: 10.1093/cvr/cvs259

20. Dobaczewski M, Chen W, Frangogiannis NG. Transforming growth factor (TGF)-β signaling in cardiac remodeling. *J Mol Cell Cardiol*. 2011;51:600–606. doi: 10.1016/j.yjmcc.2010.10.033

21. Schwanekamp JA, Lorts A, Sargent MA, York AJ, Grimes KM, Fischesser DM, Gokey JJ, Whitsett JA, Conway SJ, Molkentin JD. TGFBI functions similar to periostin but is uniquely dispensable during cardiac injury. *PLoS One*. 2017;12:e0181945. doi: 10.1371/journal.pone.0181945

22. Liguori TTA, Liguori GR, Moreira LFP, Harmsen MC. Fibroblast growth factor-2, but not the adipose tissue-derived stromal cells secretome, inhibits TGF-beta1-induced differentiation of human cardiac fibroblasts into myofibroblasts. *Sci Rep*. 2018;8:16633. doi: 10.1038/s41598-018-34747-3

23. Lim DS, Roberts R, Marian AJ. Expression profiling of cardiac genes in human hypertrophic cardiomyopathy: insight into the pathogenesis of phenotypes. *J Am Coll Cardiol*. 2001;38:1175–1180. doi: 10.1016/S0735-1097(01)01509-1